

LncRNA ASAP1-IT1 Enhances Cancer Cell Stemness via Regulating miR-509-3p/YAP1 Axis in NSCLC

Yantao Liu

Sichuan University - Wangjiang Campus: Sichuan University

Yuping Yang

Chengdu Medical College

Lingli Zhang

Sichuan University - Wangjiang Campus: Sichuan University

Jiaqiang Lin

Chengdu Medical College

Bin Li

Chengdu Medical College

Min Yang

Chengdu Medical College

Honghui Li

Aier Eye Hospital Group

Kangwu Chen

Suzhou University: Soochow University

Wei Zhao (✉ wzhao42@cityu.edu.hk)

chengdu medical college <https://orcid.org/0000-0003-2421-7311>

Research Article

Keywords: ASAP-IT1, miR-509-3p, YAP1, cancer stemness, NSCLC

Posted Date: June 28th, 2021

DOI: <https://doi.org/10.21203/rs.3.rs-445483/v2>

License:   This work is licensed under a Creative Commons Attribution 4.0 International License.

[Read Full License](#)

Abstract

Background: Non-small cell lung cancer (NSCLC) is a major cause of cancer-related death worldwide, and cancer stem cell is mainly responsible for the poor clinical outcome of NSCLC. Although previous reports indicated long noncoding RNAs (lncRNAs) play important roles in cancer stemness maintain, the underlying causes mechanisms remain is still mysterious. Our study aims to investigate the role of ASAP1 Intronic Transcript 1 (ASAP1-IT1) in cancer cell stemness of NSCLC.

Methods: qRT-PCR analysis the expression of ASAP1-IT1 and microRNA-509-3p (miR-509-3p) in NSCLC tissues, cancer cells and spheres of cancer cells-derived cancer stem cells. Knockdown of ASAP1-IT1 or overexpression of miR-509-3p in NSCLC cells by infection or transfection. Sphere formation and colony formation detects NSCLC stem cell-like properties and tumor growth *in vitro*. Luciferase reporter assays, RNA immunoprecipitation (RIP) and qRT-PCR assays analyzed the interaction between lncRNA and miRNA, qRT-PCR and Western blot detect ASAP1-IT1/miR-509-3p axis's regulation on the expression of regulated genes. NSCLC xenograft mice model validates ASAP1-IT1 role in NSCLC stemness and tumor growth *in vivo*.

Results: ASAP1-IT1 was up-regulated in NSCLC tissues, cancer cells, and in spheres of A549-derived cancer stem cells. Downregulated ASAP1-IT1 or miR-509-3p significantly decreased cell colony formation and stem cell-like properties of A549-derived stem cells with decreased expression of stem cell biomarkers SOX2, CD34, and CD133, and suppressing the expression of cell growth-related genes, Cyclin A1, Cyclin B1, and PCNA. Furthermore, knockdown of ASAP1-IT1 or overexpression of miR-509-3p repressed tumor growth in nude mice via reducing expression of tumorigenic genes. ASAP1-IT1 was found to interact with miR-509-3p. Moreover, overexpression of ASAP1-IT1 blocked miR-509-3p mediated regulation of stem cell-like properties, cell growth, and cell apoptosis of A549-derived stem cells both *in vitro* and *in vivo*. Finally, the level of YAP1 was regulated by ASAP1-IT1 and miR-509-3p.

Conclusions: YAP1-involved ASAP1-IT1/miR-509-3p axis promoted NSCLC progression by regulating cancer cell stemness and targeting related signaling is a promising therapeutic strategy to overcome NSCLC stemness.

Background

Non-small cell lung cancer (NSCLC) is the major type of lung cancer and relates the leading cause of death worldwide ¹. Although the treatment of NSCLC has been improved, the 5-years survival rate remains low owing to cancer relapse after surgery or radiotherapy ^{2,3}. Therefore, it is urgent to better understand the molecular mechanisms of NSCLC progression and find out biomarkers to identify indolent and aggressive tumors, to provide novel therapeutic strategies.

Increasing evidence have demonstrated that the recurrence of NSCLC is mostly induced by cancer stem cells in tumors ⁴⁻⁶. Cancer stem cells are involved in cancer initiation, proliferation, invasion, and

differentiation, resulting in occurrence of aggressive and metastatic cancers⁷. Simultaneously, cancer stem cells can efficiently affect multi-drug resistance in NSCLC⁸. Thus, it is an interesting and meaningful task to investigate the association of cancer stem cell and NSCLC progression, that would bring about better design of therapeutic strategies.

Long noncoding RNAs (lncRNAs) are involved in the progression of multiple cancers including NSCLC⁹⁻¹³. AFAP1-AS1 (actin filament associated protein 1) is a lncRNA which promotes NSCLC cell proliferation by epigenetically suppressing p21 expression¹⁴. Linc00673 (long intergenic non-protein coding RNA 673) modulates NSCLC cell proliferation, migration, invasion and epithelial mesenchymal transition via sponging miR-150-5p¹⁵. Linc00473 (long intergenic non-protein coding RNA 473), regulated by cAMP/CREB (adenosine monophosphate/cAMP-response element binding protein), and LKB1 (liver kinase B1) inhibits lung cancer and controls tumor growth¹⁶. Furthermore, lncRNAs also affect the stemness of lung cancer cells. DGC5 (DiGeorge syndrome critical region gene 5) contributes to cancer cell stemness-like properties by regulating miR-330-5p/CD44 in NSCLC¹⁷. Linc00662 (long intergenic non-protein coding RNA 662) increases cancer stem cell-like phenotypes in lung cancer¹⁸. FENDFRR (FOXF1 adjacent non-coding developmental regulatory RNA) inhibits cancer cell stemness by repressing expression of MDR1 (multi-drug resistance gene 1) by interacting with the RNA binding protein HuR in NSCLC development¹⁹. Linc-ITGB1 (long intergenic non-protein coding RNA integrin subunit beta 1) decreases cancer stemness via down-regulating Snail in NSCLC²⁰. HAND2-AS1 (heart and neural crest derivatives expressed 2 antisense RNA 1) elevates cancer cell stemness of lung cancer cells via binding with TGF-beta1 (transforming growth factor beta1)²¹. Interestingly, lncRNA ASAP1-IT1 (ArfGAP with SH3 domain, ankyrin repeat and PH domain 1 intronic transcript 1) increases cell proliferation, invasion, and metastasis by regulating PTEN/AKT (phosphatase and tensin homolog/AKT serine/threonine kinase 1) axis in NSCLC²². ASAP1-IT1 enhances stemness and overexpression of ASAP1-IT1 indicates a poor prognosis in patients with bladder cancer²³. In addition, ASAP1-IT1 promotes development of cholangiocarcinoma through hedgehog signaling pathway²⁴. However, the role of ASAP1-IT1 on cancer cell stemness in NSCLC is largely unknown.

We explored the role of ASAP1-IT1 in NSCLC progression. The binding of ASAP1-IT1 with miRNAs was predicted using LncBook database (a curated knowledgebase of human long non-coding RNAs) (<https://bigd.big.ac.cn/lncbook/index>). We found that miR-509-3p was a potential target of ASAP1-IT1. MiR-509-3p functions as a tumor suppressor demonstrated by the previous studies. For instance, miR-509-3p increases platinum drug sensitivity to induce cell apoptosis in ovarian cancer^{25,26}. MiR-509-3p suppresses cell proliferation and migration by up-regulating XIAP (X-linked inhibitor of apoptosis) in gastric cancer²⁷. MiR-509-3p represses cell proliferation and invasion by decreasing XIAP in glioma²⁸. MiR-509-3p is down-regulated by the oncoprotein HBXIP (late endosomal/lysosomal adaptor, MAPK and MTOR activator 5) via activating NF-κB in hepatoma cells. Additionally, the potential targets of miR-509-3p were predicted using Target Scan tools, and the results showed that YAP1 (Yes associated protein 1) was a downstream target of miR-509-3p in NSCLC cells. YAP1 has been considered as an oncogene in

multiple cancers including NSCLC^{29–33}. YAP1 positively regulates drug resistance and cancer cell stemness^{29,30}. Also, YAP1 is the main effector of the Hippo signaling pathway involved in human cancers³⁴.

In this study, we investigate the role of ASAP1-IT1, and the association of ASAP1-IT1, miR-509-3p and YAP1 in NSCLC progression and cancer cell stemness.

Materials And Methods

Clinical specimens

NSCLC specimens were collected from 94 patients who were treated in the First Affiliated Hospital of Chengdu Medical College (Chengdu, China) from April in 2019 to September in 2020. The collection of clinical samples was approved by the ethics committee of Chengdu Medical College (approved ID: BR20re19), and each participant signed an informed consent form. All the patients were given no treatment before surgery. The collected specimens were stored in a liquid nitrogen tank.

Cell maintenance and transfection

The A549 and A549/R (cisplatin resistant) cells were obtained from China Infrastructure of Cell Line Resource (Beijing, China), and cultured in DMEM (Dulbecco's Modified Eagle Medium) media (WISENT, Nanjing, Jiangsu, China) in a CO₂ incubator at 37 °C. The DMEM media was supplemented with 10% FBS (fetal bovine serum), 100 mg/mL streptomycin and 100 U/mL penicillin (WISENT). The FBS was bought from Thermo Fisher Scientific (Waltham, Massachusetts, USA). All the other cell culture materials were bought from WISENT.

The cell infection was conducted according to its instruction book (Genechem, Shanghai, China). sh-ASAP1-IT1: 5'-GCU GCG ACA AUA GAC AUC GGA GUU U-3', and sh-NC: 5'-CUC UCG GAA CAU GUC ACA U-3'. The mimic microRNAs and inhibitors were purchased from Ribobio (Guangzhou, China), miR-509-3p-related sequences were listed, Mock, 5'-UCU CCG AAC GUG UCA CGU U-3'; and anti-miR-509-3p, 5'-CCG UGG UUC AUA CUG GUA-3'; miR-509-3p mimic, 5'-UAC CAC AGG GUA GAA CCA CGG-3'. The pmirGLO-ASAP1-IT1-WT (wild type) or -Mut (Mutant), and pmirGLO-Yap1-3'UTR (untranslated region)-WT or -Mut (Mutant), and pcDNA-sh-NC, pcDNA-sh-ASAP1-IT1 were from Thermo Fisher Scientific.

Hematoxylin-eosin (H&E) staining

The NSCLC specimens were fixed in 4% paraformaldehyde, embedded in paraffin and subjected to sectioning. Then, H & E staining was performed as described previously¹⁰. All the chemicals and reagents were bought from Servicebio (Wuhan, Hubei, China).

RNA extraction and qRT-PCR (quantitative real time polymerase chain reaction)

The total RNA was extracted using TRIzol reagent (Life Technologies, Rockville, MD, USA). The reverse transcription kit (Thermo Fisher Scientific) was applied to synthesize cDNA (complementary DNA) from the total RNA. Quantitative RT-PCRs were used to evaluate the levels of miRNAs, lncRNAs, or mRNAs using the SYBR Premix Ex Taq II (TaKaRa, Dalian, China). The qRT-PCR was carried out under the thermal cycling conditions: 95 °C × 5 min, and 40 cycles of 95 °C × 30 s, 60 °C × 30 s, and 72 °C × 1 min. GAPDH (glyceraldehyde-3-phosphate dehydrogenase) was used as the internal control for RNA and lncRNA, U6 was used as the internal control of miRNAs. The relative RNA levels were calculated following the $2^{-\Delta\Delta CT}$ method. The PCR primers were as follows: U6, 5'-TGC GGG TGC TCG CTT CGG CAG C-3' (forward), 5'-GTG CAG GGT CCG AGG T-3' (reverse); miR-509-3p, 5'-UAC CAC AGG GUA GAA-3' (forward), 5'-CTCTACAGCTATATTGCCAGCCA-3' (reverse); GAPDH, 5'-CAC CCA CTC CTC CAC CTT TG-3' (forward), 5'-CCA CCA CCC TGT TGC TGT AG-3' (reverse); Cyclin A1, 5'-ATAACGACGGGAAGAGCGG-3' (forward), 5'-CAGGGTACATGATTGCGGGA-3' (reverse); Cyclin B1, 5'-CAGGTTGTTGCAGGAGACCA-3' (forward), 5'-CATGGCAGTGACACCAACCA-3' (reverse); PCNA (proliferating cell nuclear antigen), 5'-CGCCCTGGTTCTGGAGGTAA-3' (forward), 5'-GGCTGAGACTTGCGTAAGGG-3' (reverse); Bcl-2, 5'-TTCTTTGAGTTCGGTGGGGT-3' (forward), 5'-GAAATCAAACAGAGGCCGCAT-3' (reverse); Bax, 5'-GGG TTG TCG CCC TTT TCT AC-3' (forward), 5'-AGT CGC TTC AGT GAC TCG G-3' (reverse); caspase-3, 5'-GGGGAGCTTGGAACGGTACG-3' (forward), 5'-CCACTGACTTGCTCCCATGTAT-3' (reverse); YAP1, 5'-TGCTGTCCCAGATGAACGTC-3' (forward), 5'-GGTTCATGGCAAACGAGGG-3' (reverse); ASAP1-IT1, 5'-AAACATCATCCCCAGAGTGG-3' (forward), 5'-GCCTTGCTCACCTCTGAAAC-3' (reverse); SOX2 (SRY-box transcription factor 2), 5'-CAT GAA GGA GCA CCC GGA TT-3' (forward), 5'-ATG TGC GCG TAA CTG TCC AT-3' (reverse); CD44, 5'-GCC ACC AGA GCT ATT CCC AA-3' (forward), 5'-GGT CTT CGC CCA GCC TTT CT-3' (reverse); CD133, 5'-GCC ATG CTC TCA GCT CTC C-3' (forward), 5'-TCC TGA AAA GGA GTT CCC GC-3' (reverse). All experiments were performed in quadruplicate, and each assay was repeated independently for 3 times.

Western blot

Total protein samples were prepared from the tissues or cells using RIPA (radio immunoprecipitation assay) buffer (Beyotime) for 30 min. The lysates were centrifuged at 12,000 g for 15 min to obtain the supernatants, and they were de-natured at 98 °C for 20 min. 50 µg proteins were used for sodium dodecyl sulfate-polyacrylamide gel electrophoresis (SDS-PAGE) (Bio-Rad, Hercules, CA, USA). All the prepared gels were transferred to the 0.22 µm PVDF (polyvinylidene difluoride) membranes (Thermo Fisher Scientific) for 2 h, and the proteins-carried PVDF were blocked with 1% bovine serum albumin. Then, the PVDF membranes were incubated with the primary antibody overnight in a 4 °C refrigerator. The membranes were incubated with the HRP (horseradish peroxidase)-conjugated secondary antibody diluted at 1: 50 000 (Bioworld Technology, Nanjing, China) for 1 hour. The anti-YAP1 and anti-Tubulin- α were bought from Thermo Fisher Scientific.

Sphere formation and colony formation of cancer stem cells

Cancer stem cells were sorted from A549 cells or transfected-A549 cells by spherocyst medium¹⁰. The 3×10^4 cells were seeded in 6-well ultra-low cluster plates (Thermo Fisher Scientific). They were maintained in DMEM/F12 serum free medium (Thermo Fisher Scientific) containing epidermal growth factor (20 ng/mL), beta-fibroblast growth factor (20 ng/mL), insulin (4 μ g/mL), and B27 (2%). All reagents were from Sigma. Finally, the number of spheres was counted under an inverted microscope (Leica, Oskar-Barnack-StraÙe, Germany) post 10 days incubation. The biomarkers of cancer stem cells SOX2, CD34, and CD133 were used to identify the cancer stem cells using qRT-PCR and Western blot.

The A549 cancer stem cells were isolated using magnetic bead kit, and 3×10^4 stem cells were seeded in six-well plates with ultra-low adhesion. They were cultured in sphere formation media for a week, and post another 20 days, the number of spheres was calculated under a microscope.

Cell apoptosis and cell cycle analysis

To determine cell apoptosis of A549-derived stem cells and other cells, cells were collected at $80 \times 4^\circ\text{C} \times 5$ min for annexin-V/FITC (fluoresceine isothiocyanate)/PI (propidium iodide) staining after 48 h infection with the indicated plasmids or miRNAs. Briefly, cells were incubated with annexin-V and PI for 10 min and 5 min, respectively, in a dark room using the annexin V-FITC/PI staining kit (Beyotime, Beijing, China). Finally, the cell cycle was evaluated using Beckman Coulter Navios EX flow cytometry (Beckman, Shanghai, China).

For analyzing cell cycle, the cells were cultured in 12-well plates (Thermo Fisher Scientific). After transfection with the indicated miRNAs or plasmids for 48 h, they were subjected to suspension and fixation in 75% ethanol at 4°C for 12 h. Then, they were washed with PBS (phosphate-buffered saline) for 3 times. Afterwards, they were resuspended in 500 μ L staining buffer containing propidium iodide (5 mg/ml)/RNase (10 mg/ml) at 37°C for 30 min in a dark room. Finally, cell apoptosis rate was evaluated using the flow cytometry. Each treatment group consisted four wells, and each assay was repeated for 3 times independently.

Cell counting kit-8 (CCK-8) assay

The A549-derived stem cells or A549 cells were plated into a 96-well plate (Thermo Fisher Scientific) at the density of 4×10^3 cells per well for determination of cell viability. CCK-8 reagent (Sangon, Shanghai, China) were added into medium when cultured 36 h. After incubation for 1 h at 37°C , the formation of water-soluble formazan was examined in a microplate reader (Bio-Rad) with the light length of 450 nm. All experiments were performed in quadruplicate, and each assay was repeated independently for 3 times.

Dual luciferase reporter assay

To determine the effects of miR-509-3p on luciferase activity of pmirGLO-ASAP1-IT1, 2×10^4 A549 cells per well were seeded in 24-well plates. They were co-transfected with pmirGLO-ASAP1-IT1-WT (wild type),

pmirGLO-ASAP1-IT1-Mut (Mutant), as well as Mock (negative control), miR-509-3p mimic, and anti-miR-509-3p. To examine the effects of miR-509-3p on luciferase activity of pmirGLO-Yap1-3'UTR, the cells were co-transfected with pmirGLO-Yap1-3' UTR-WT, pmirGLO-Yap1-3' UTR-Mut (Mutant), as well as Mock, miR-509-3p mimic, and anti-miR-509-3p. After transfection for 48 h, they were collected and lysed. The supernatants were used for measurement of luciferase activity using the Dual-Luciferase Assay Kit on GloMax 20/20 Luminometer following the manufacturer's instructions (Promega, Madison, USA). All experiments were performed in quadruplicate, and each assay was repeated independently for 3 times.

RNA immunoprecipitation (RIP) assay

RIP assay was conducted to examine the interaction between ASAP1-IT1 and miR-509-3p using the RIP RNA-binding protein immunoprecipitation kit Magna (Millipore, Massachusetts, USA). Briefly, the cell lysate was incubated with anti-Ago2 (argonaute-2), and anti-IgG was used as a negative control. The antibodies were purchased from Bioworld Technology (Nanjing, China). At last, the collected immunoprecipitated RNA samples were used to determine ASAP1-IT1 and miR-1301-3p content by qRT-PCR analysis. All experiments were performed in quadruplicate, and each assay was repeated independently for 3 times.

Mouse tumorigenesis assay

The A549-derived stem cells were infected with the mentioned shRNAs or plasmids as indicated. Post 48 h infection, the A549-derived stem cells were collected at $80\text{ g} \times 4\text{ }^{\circ}\text{C} \times 5\text{ min}$. Afterwards, 4×10^6 cells were inoculated into 5-week-old nude mice. The BALB/c nude mice were bought from the Model Animal Research Center of Nanjing University (Nanjing, China), and divided randomly for each group (3 mice for each group). The animal experiments were approved by the research ethics committee of Chengdu Medical College (approved animal protocol No.: CMC20LM22). The tumor volume was calculated every 3 days using the formula, tumor volume = $(\text{length} \times \text{width}^2)/2$. All the tumor-carried nude mice were euthanized by CO₂ exposure as described previous report³⁵ on the 24th day post inoculation.

Statistical analysis

Statistical analysis was conducted using SPSS software package (version 20.0, SPSS Inc., NY, USA) and GraphPad Prism 6 (GraphPad Software, CA, USA), and p value < 0.05 was statistically significant. The data were obtained from three independent experiments, and all data are expressed as mean \pm standard deviation (S.D.). The statistical significance was examined using Two-tailed Student's t-test for two-group comparisons and one-way analysis of variance (ANOVA) test with post-hoc analysis for multi-group comparisons.

Results

ASAP1-IT1 is overexpressed in NSCLC tissues and knockdown of ASAP1-IT1 inhibited stemness of NSCLC cells

To evaluate the role of ASAP1-IT1 in NSCLC, we determined the ASAP1-IT1 expression in human NSCLC specimens and adjacent tissues using qRT-PCR. The H&E staining confirmed the dysregulated cancerous growth in NSCLC tissues (Figure 1A). The qRT-PCR results demonstrated that ASAP1-IT1 was significantly overexpressed in NSCLC tissues compared with that in adjacent tissues (Figure 1B). ASAP1-IT1 was also up-regulated in NSCLC cells (A549, Calu-3, PC-9, and SPCA-1) (Figure 1C). To investigate the role of ASAP1-IT1 in inducing stemness in NSCLC, we determined the ASAP1-IT1 expression between parental A549 cells and stemness-enriched A549 spheres. The qRT-PCR data showed that ASAP1-IT1 was markedly elevated in spheres of A549-derived stem cells compared with the parental group (Figure 1D). Meanwhile, stemness-associated genes including SOX2, CD44, CD133 were increased in A549 spheres compared with that in parental cells (Figure 1E). To explore the function of ASAP1-IT1 in stemness formation, the ASAP1-IT1 expression was knocked down in A549-derived stem cells (Figure 1F). The qRT-PCR analysis showed that knockdown of ASAP1-IT1 significantly down-regulated expression of stemness-associated genes SOX2, CD44, and CD133 in A549-derived stem cells (Figure 1G). Furthermore, suppression of ASAP1-IT1 significantly reduced sphere formation in comparison to the pcDNA-sh-NC group (Figure 1H, I). Additionally, downregulation of ASAP1-IT1 also arrested A549-derived stem cells in G0/G1 phase (Figure 1J).

Knockdown of ASAP1-IT1 suppressed cell growth and reduced cisplatin resistance in cancer stem cells, and promoted apoptosis

Cancer stem cells (CSCs) are closely associated with chemo-resistance, which often reduces therapeutic effects of anti-cancer drugs, such as cisplatin. To examine whether ASAP1-IT1 serves as a dominant factor of cisplatin resistance in NSCLC cells, A549 cells with ASAP1-IT1-knockdown were incubated with 4 μ M cisplatin. The qRT-PCR data exhibited that ASAP1-IT1 was increased after incubation with cisplatin in a time-dependent manner (Figure 2A). Also, ASAP1-IT1 was up-regulated in A549/R cells compared with that in A549 cells (Figure 2B). ASAP1-IT1-knockdown A549 cells were then incubated with cisplatin at different concentration, and the CCK-8 assays demonstrated that increasing concentration of cisplatin significantly decreased cell viability of A549 cells with ASAP1-IT1-knockdown (Figure 2C). Moreover, annexin V-FITC/PI assays and qRT-PCR analysis confirmed that ASAP1-IT1 knockdown obviously increased apoptotic cells of A549 by elevating expression of Bax and caspase-3, and inhibiting Bcl-2 expression (Figure 2D-F). Knockdown of ASAP1-IT1 also repressed colony formation of A549-derived stem cells (Figure 2G, H), and silencing ASAP1-IT1 expression significantly decreased expression of cell growth-associated genes including Cyclin A1, Cyclin B1, and PCNA (Figure 2I).

ASAP1-IT1 reciprocally interacted with miR-509-3p

To find out the molecular mechanisms of ASAP1-IT1 in regulating NSCLC progression, we predicted its potential interaction with miRNAs using LncBook database (a curated database of human long non-coding RNAs) (<https://bigd.big.ac.cn/lncbook/index>). It was found that miR-509-3p might be a target miRNA of ASAP1-IT1 (Figure 3A). In the meantime, miR-509-3p was found to be downregulated in NSCLC tissues, and its expression was negatively correlated with ASAP1-IT1 (Figure 3B, C). In addition, ASAP1-

IT1 significantly suppressed miR-509-3p expression in A549 cells (Figure 3D). Furthermore, miR-509-3p inhibited luciferase activity of pmirGLO-ASAP1-IT1-WT, and miR-509-3p failed to affect the luciferase activity of pmirGLO-ASAP1-IT1-Mut, which contained the mutated binding sites of miR-509-3p on ASAP1-IT1 (Figure 3E, F). Moreover, overexpression of miR-509-3p repressed ASAP1-IT1 level while inhibition of miR-509-3p elevated ASAP1-IT1 expression (Figure 3G). To confirm the direct interaction between miR-509-3p and ASAP1-IT1, RIP assay was conducted. The results supported that ASAP1-IT1 could interact with miR-509-3p in A549 cells (Figure 3H).

Overexpression of miR-509-3p inhibited stemness, cisplatin resistance and cell growth of A549 stem cells, and promoted apoptosis

The roles of miR-509-3p in stemness, cisplatin resistance, cell growth, and cell apoptosis were investigated both *in vitro* and *in vivo*. Quantitative RT-PCR analysis demonstrated that miR-509-3p was reduced in spheres of A549 compared with the parental group (Figure 4A). Meanwhile, overexpression of miR-509-3p significantly inhibited stemness-associated genes SOX2, CD44, and CD133 in A549-derived stem cells compared with that in Mock group (Figure 4B). Overexpression of miR-509-3p suppressed sphere formation in comparison to Mock-transfected A549-derived stem cells (Figure 4C, D). MiR-509-3p markedly arrested A549-derived stem cells in G0/G1 phase (Figure 4E). MiR-509-3p was decreased in A549/R cells compared with A549 cells (Figure 4F) hints that miR-509-3p functions as an essential regulator of chemo-resistance in NSCLC cells. Furthermore, miR-509-3p-overexpressed A549-derived stem cells were incubated with cisplatin at different concentration, and CCK-8 assays showed that increasing concentration of cisplatin significantly decreased cell viability of miR-509-3p-overexpressed A549-derived stem cells (Figure 4G). Annexin V-FITC/PI assays and qRT-PCR analysis showed that miR-509-3p-overexpression markedly elevated apoptosis of A549-derived stem cells by promoting expression of Bax and caspase-3, and down-regulating Bcl-2 expression (Figure 4H, I, J). Furthermore, miR-509-3p-overexpression significantly decreased colony formation of A549-derived stem cells by inhibiting expression of cell growth-associated genes Cyclin A1, Cyclin B1, and PCNA (Figure 4K, L, M).

Overexpression of ASAP1-IT1 blocked miR-509-3p-mediated cell functions of cancer stem cells both *in vitro* and *in vivo*.

Based on the above results, overexpression of miR-509-3p reduced the stemness, cisplatin resistance and growth, and promoted apoptosis of A549-derived stem cells both *in vitro* and *in vivo*. Analysis of sphere formation indicated that overexpression of ASAP1-IT1 significantly overturned miR-509-3p-mediated less number and smaller size sphere formation and restored expression of stemness-associated genes including SOX2, CD44, and CD133 (Figure 5A, B). ASAP1-IT1 overexpression reversed miR-509-3p-induced apoptosis by restoring miR-509-3p-controlled expression of apoptotic genes (Figure 5C, D). Similarly, ASAP1-IT1 overexpression abolished miR-509-3p-suppressed cell growth by recovering miR-509-3p-mediated expression of cell growth-related genes including Cyclin A1, Cyclin B1, and PCNA (Figure 5E, F).

Moreover, *in vivo* xenografts were found that overexpression of miR-509-3p significantly decreased tumor growth whereas overexpression of ASAP1-IT1 could block miR-509-3p-mediated inhibitory activity on

tumor growth (Figure 5G, H, I). Finally, ASAP1-IT1 also reversed miR-509-3p-controlled expression of genes involved in stemness, cell growth, and cell apoptosis in tumors (Figure 5J).

YAP1 is regulated by miR-509-3p and ASAP1-IT1

To further explore the potential molecular mechanism of ASAP1-IT1 and miR-509-3p interaction in NSCLC progression, we explored the downstream molecule of miR-509-3p using online bioinformatics analysis. YAP1 was identified as a target gene of miR-509-3p (Figure 6A). YAP1 was elevated in NSCLC tissues compared with that in adjacent tissues by qRT-PCR analysis (Figure 6B). Meanwhile, qRT-PCR analysis also revealed that YAP1 was up-regulated in spheres compared with adherent cancer cells (Figure 6C). Luciferase reporter assay demonstrated that miR-509-3p suppressed luciferase activity of pmirGLO-YAP1-3'UTR-WT, and it failed to affect the luciferase activity of pmirGLO-YAP1-3'UTR-Mut which contained the mutated binding sites of miR-509-3p on YAP1 3'UTR (Figure 6D). In addition, overexpression of miR-509-3p significantly reduced YAP1 expression at the mRNA and protein levels (Figure 6E, F). Moreover, overexpression of ASAP1-IT1 enhanced YAP1 expression (Figure 6D, E, F), and significantly blocked miR-509-3p-controlled YAP1 expression evidenced by luciferase reporter assay, qRT-PCR, and Western blot (Figure 6D, E, F).

Overexpression of YAP1 reversed miR-509-3p function on cancer stemness, cell growth, and apoptosis in A549-derived stem cells

To determine whether YAP1 is required for the function of miR-509-3p, we overexpressed YAP1 and miR-509-3p in A549-derived stem cells. It was found that overexpression of YAP1 reversed the inhibitory effect of miR-509-3p on stemness evidenced by sphere formation and restoring expression of stemness-associated genes SOX2, CD44, and CD133 in A549-derived stem cells (Figure 7A, B). Overexpression of YAP1 significantly attenuated miR-509-3p-induced apoptosis by restoring miR-509-3p-controlled expression of apoptotic genes Bax, Bcl-2, caspase-3 (Figure 7C, D). Furthermore, YAP1 overexpression abolished miR-509-3p-suppressed cell growth of A549-derived stem cells via recovering expression of cell growth-related genes Cyclin A1, Cyclin B1, and PCNA (Figure 7E, F).

Discussion

Increasing evidence have demonstrated that cancer stem cells participate in the aggressive and destructive behaviors of lung cancers including NSCLC, a main cause of cancer-induced death worldwide^{2,3,36,37}. The cancer stem cells significantly increase the recurrence of NSCLC post surgery or radiotherapy⁴⁻⁶. The cancer stem cells possess the properties of self-renewal, cancer initiation, and cancer progression⁷. Cancer stem cells also aggravate multi-drug resistance in lung cancer⁸. Therefore, exploring cancer stem cell-related potential molecular mechanism in NSCLC progression is critical, as it would contribute to the treatment of patients with NSCLC.

It has been reported that a variety of lncRNAs are involved in the progression of NSCLC^{14,15,38,39}. As previously reported, ASAP1-IT1 is upregulated in NSCLC and promotes cancer proliferation, invasion and

migration²². Consistent with this report, we observed that ASAP1-IT1 was up-regulated in NSCLC tissues, cancer cells, and A549 cell spheres. ASAP1-IT1 was also overexpressed in A549/R cells, suggesting that ASAP1-IT1 could be associated with cisplatin resistance. Knockdown of ASAP1-IT1 significantly inhibited cancer stem cell colony formation and cancer cell stemness of A549 cells. Further studies demonstrated that knockdown of ASAP1-IT1 suppressed expression of stem cell biomarkers SOX2, CD34, and CD133 in A549-derived stem cells. Then, downregulating ASAP1-IT1 expression decreased expression of cell growth-associated genes Cyclin A1, Cyclin B1, and PCNA, and elevated expression of cell apoptosis related genes Bax and caspase-3 and reduced anti-apoptotic Bcl-2 expression in A549-derived stem cells. The *in vivo* experiments proved that knockdown of ASAP1-IT1 significantly inhibited tumor growth in nude mice. Thus, these *in vitro* and *in vivo* findings suggested that ASAP1-IT1 act as an oncogene to regulate cancer cell stemness, cell growth and cell apoptosis in NSCLC. Down-regulation of ASAP1-IT1 could be a good strategy to fight against NSCLC.

LncRNAs exert their activity in cancers often by functioning as sponges of miRNAs^{15,40}. In this study, ASAP1-IT1 may directly interact with miR-509-3p in NSCLC cells. Previous studies have revealed that miR-509-3p inhibit tumor growth in multiple types of cancers. For example, miR-509-3p improves sensitivity of cancer cells to platinum in ovarian cancer^{23,24}, and it depresses cell proliferation and invasion via down-regulating X-linked inhibitor of apoptosis in glioma²⁸. MiR-509 promotes hepatoma progression by activating NF- κ B (nuclear factor kappa B) signaling pathway. However, the role of miR-509-3p in the stemness of NSCLC has not been investigated. In consistent with previous studies, miR-509-3p was significantly down-regulated in NSCLC tissues, NSCLC cells, A549 spheres, and in A549/R cells. Overexpression of miR-509-3p suppressed sphere formation and cell growth, and increased cell apoptosis of A549-derived stem cells. Also, overexpression of miR-509-3p decreased expression of SOX2, CD44, and CD133, and enhanced expression of Bax and caspase-3 while repressed Bcl-2 expression in cancer cells. Furthermore, overexpression of miR-509-3p suppressed tumor growth in nude mice. These results implied that miR-509-3p was a tumor suppressor, and overexpression of miR-509-3p could offer a novel approach to prevent NSCLC progression. Furthermore, overexpression of ASAP1-IT1 significantly blocked overexpression of miR-224-3p-mediated inhibition of cancer stem cell-like properties and cell growth of A549-derived stem cells both *in vitro* and *in vivo*. Additionally, overexpression of ASAP1-IT1 abolished miR-509-3p-induced cancer cell apoptosis of A549-derived stem cells both *in vitro* and *in vivo*, indicating that the interaction between ASAP1-IT1 and miR-509-3p is involved in regulation of cancer cell stemness and NSCLC progression.

Bioinformatics analysis showed that miR-509-3p could target the 3'UTR of YAP1, which is an oncogene in the Hippo signaling pathway involved in human cancers³⁴. Our study indicated that overexpression of YAP1 rescued miR-509-3p-mediated anti-cancer activities, suggesting that miR-509-3p exhibit its activities partly depending on YAP1 expression. Our results were in consistent with the previous studies which supported that YAP1 is an oncogene and aggravates drug resistance and cancer cell stemness in NSCLC^{29-33,41,42}. Moreover, we also observed that interaction of ASAP1-IT1 with miR-509-3p led to

reciprocally inhibition. These findings demonstrated that YAP1 is involved in ASAP1-IT1/miR-509-3p interaction and plays an important role in cancer cell stemness and progression of NSCLC.

Conclusion

In conclusion, ASAP1-IT1 is up-regulated in NSCLC and promotes cancer cell stemness by suppressing miR-509-3p. YAP1 is modulated by ASAP1-IT1 and miR-509-3p in A549-derived stem cells. ASAP1-IT1 and miR-509-3p could be potential therapeutic targets of NSCLC.

Abbreviations

ASAP1-IT1: ASAP1 Intronic Transcript 1; NSCLC: Non-small cell lung cancer; CSCs: Cancer stem cells; lncRNAs: long noncoding RNAs; miR-509-3p: microRNA-509-3p; RIP: RNA immunoprecipitation; H&E: Hematoxylin-eosin; CCK-8: Cell counting kit-8; Linc00673/00473: long intergenic non-protein coding RNA 673/00473; cAMP/CREB: adenosine monophosphate/cAMP-response element binding protein; LKB1: liver kinase B1; DGC5: DiGeorge syndrome critical region gene 5; FENDFRR: FOXF1 adjacent non-coding developmental regulatory RNA; MDR1: multi-drug resistance gene 1; PTEN/AKT: phosphatase and tensin homolog/AKT serine/threonine kinase 1; XIAP: X-linked inhibitor of apoptosis; YAP1: Yes associated protein 1.

Declarations

Acknowledgements

We acknowledge the language edition by UNIWINSCI. Inc, and thank the patients enrolled in this study.

Authors' contributions

W.Z., K.C. and Y.L. conceived and designed the study. Y.Y., Y.L., L.Z., J.L., H.L. and B.L. performed experiments. J.L., M.Y. and B.L. searched the literature. W.Z. and K.C. performed data extraction and analysis. W.Z. and K.C. drafted the manuscript. All authors revised and approved the final manuscript.

Fundings

This work was supported by the National Natural Science Foundation of China (81602636 and 81802682), Nanjing medical science and technology development project (ZKX15049), Key project of science of Sichuan Education Department (18ZA0164), Natural Science Foundation of Chengdu Medical College (CYZ18-04), the Natural Science Foundation of Jiangsu Province (BK 20180199) and Miaozi project of science and Technology Department of Sichuan Province (2018RZ0095).

Availability of data and materials

The datasets supporting the conclusions of this article are included within the article and could be obtained from the corresponding author if necessary.

Ethics approval and consent to participate

This specimen collection was approved by the Ethics Committee of Chengdu Medical College (approved ID: BR20re19), and each participant signed an informed consent form. The animal experiments were approved by the Research Ethics Committee of Chengdu Medical College (approved animal protocol No.: CMC20LM22).

Consent for publication

Not applicable.

Competing interests

The authors declare that they have no competing interests.

References

1. Sung H, Ferlay J, Siegel RL, et al. Global cancer statistics 2020: GLOBOCAN estimates of incidence and mortality worldwide for 36 cancers in 185 countries. *CA: a cancer journal for clinicians*. 2021.
2. Chen W, Zheng R, Baade PD, et al. Cancer statistics in China, 2015. *CA Cancer J Clin*. 2016;66(2):115-132.
3. Wood SL, Pernemalm M, Crosbie PA, Whetton AD. Molecular histology of lung cancer: from targets to treatments. *Cancer treatment reviews*. 2015;41(4):361-375.
4. Auperin A, Le Pechoux C, Rolland E, et al. Meta-analysis of concomitant versus sequential radiochemotherapy in locally advanced non-small-cell lung cancer. *Journal of clinical oncology : official journal of the American Society of Clinical Oncology*. 2010;28(13):2181-2190.
5. Sourisseau T, Hassan KA, Wistuba I, et al. Lung cancer stem cell: fancy conceptual model of tumor biology or cornerstone of a forthcoming therapeutic breakthrough? *Journal of thoracic oncology : official publication of the International Association for the Study of Lung Cancer*. 2014;9(1):7-17.
6. Kitamura H, Okudela K, Yazawa T, Sato H, Shimoyamada H. Cancer stem cell: implications in cancer biology and therapy with special reference to lung cancer. *Lung cancer*. 2009;66(3):275-281.
7. Reya T, Morrison SJ, Clarke MF, Weissman IL. Stem cells, cancer, and cancer stem cells. *Nature*. 2001;414(6859):105-111.
8. Singh A, Settleman J. EMT, cancer stem cells and drug resistance: an emerging axis of evil in the war on cancer. *Oncogene*. 2010;29(34):4741-4751.

9. Li C, Zhao W, Pan X, et al. LncRNA KTN1-AS1 promotes the progression of non-small cell lung cancer via sponging of miR-130a-5p and activation of PDPK1. *Oncogene*. 2020;39(39):6157-6171.
10. Yan F, Zhao W, Xu X, et al. LncRNA DHRS4-AS1 Inhibits the Stemness of NSCLC Cells by Sponging miR-224-3p and Upregulating TP53 and TET1. *Frontiers in cell and developmental biology*. 2020;8:585251.
11. Shao G, Zhao Z, Zhao W, et al. Long non-coding RNA MALAT1 activates autophagy and promotes cell proliferation by downregulating microRNA-204 expression in gastric cancer. *Oncology letters*. 2020;19(1):805-812.
12. Huang N, Guo W, Ren K, et al. LncRNA AFAP1-AS1 Suppresses miR-139-5p and Promotes Cell Proliferation and Chemotherapy Resistance of Non-small Cell Lung Cancer by Competitively Upregulating RRM2. *Frontiers in oncology*. 2019;9:1103.
13. Song J, Wu X, Ma R, Miao L, Xiong L, Zhao W. Long noncoding RNA SNHG12 promotes cell proliferation and activates Wnt/beta-catenin signaling in prostate cancer through sponging microRNA-195. *Journal of cellular biochemistry*. 2019;120(8):13066-13075.
14. Yin D, Lu X, Su J, et al. Long noncoding RNA AFAP1-AS1 predicts a poor prognosis and regulates non-small cell lung cancer cell proliferation by epigenetically repressing p21 expression. *Molecular cancer*. 2018;17(1):92.
15. Lu W, Zhang H, Niu Y, et al. Long non-coding RNA linc00673 regulated non-small cell lung cancer proliferation, migration, invasion and epithelial mesenchymal transition by sponging miR-150-5p. *Mol Cancer*. 2017;16(1):118.
16. Chen Z, Li JL, Lin S, et al. cAMP/CREB-regulated LINC00473 marks LKB1-inactivated lung cancer and mediates tumor growth. *J Clin Invest*. 2016;126(6):2267-2279.
17. Wang R, Dong HX, Zeng J, Pan J, Jin XY. LncRNA DGCR5 contributes to CSC-like properties via modulating miR-330-5p/CD44 in NSCLC. *J Cell Physiol*. 2018;233(9):7447-7456.
18. Gong W, Su Y, Liu Y, Sun P, Wang X. Long non-coding RNA Linc00662 promotes cell invasion and contributes to cancer stem cell-like phenotypes in lung cancer cells. *Journal of biochemistry*. 2018;164(6):461-469.
19. Gong F, Dong D, Zhang T, Xu W. Long non-coding RNA FENDRR attenuates the stemness of non-small cell lung cancer cells via decreasing multidrug resistance gene 1 (MDR1) expression through competitively binding with RNA binding protein HuR. *European journal of pharmacology*. 2019;853:345-352.
20. Guo L, Sun C, Xu S, et al. Knockdown of long non-coding RNA linc-ITGB1 inhibits cancer stemness and epithelial-mesenchymal transition by reducing the expression of Snail in non-small cell lung cancer.

Thoracic cancer. 2019;10(2):128-136.

21. Miao F, Chen J, Shi M, Song Y, Chen Z, Pang L. LncRNA HAND2-AS1 inhibits non-small cell lung cancer migration, invasion and maintains cell stemness through the interactions with TGF-beta1. *Bioscience reports*. 2019;39(1).
22. Zhang L, Shi SB, Zhu Y, Qian TT, Wang HL. Long non-coding RNA ASAP1-IT1 promotes cell proliferation, invasion and metastasis through the PTEN/AKT signaling axis in non-small cell lung cancer. *European review for medical and pharmacological sciences*. 2018;22(1):142-149.
23. Yang L, Xue Y, Liu J, et al. Long noncoding RNA ASAP1-IT1 promotes cancer stemness and predicts a poor prognosis in patients with bladder cancer. *Neoplasma*. 2017;64(6):847-855.
24. Guo L, Zhou Y, Chen Y, Sun H, Wang Y, Qu Y. LncRNA ASAP1-IT1 positively modulates the development of cholangiocarcinoma via hedgehog signaling pathway. *Biomed Pharmacother*. 2018;103:167-173.
25. Niu L, Ni H, Hou Y, Du Q, Li H. miR-509-3p enhances platinum drug sensitivity in ovarian cancer. *Gene*. 2019;686:63-67.
26. Chen W, Du J, Li X, et al. miR-509-3p promotes cisplatin-induced apoptosis in ovarian cancer cells through the regulation of anti-apoptotic genes. *Pharmacogenomics*. 2017;18(18):1671-1682.
27. Sun J, Li J, Zhang W, et al. MicroRNA-509-3p Inhibits Cancer Cell Proliferation and Migration via Upregulation of XIAP in Gastric Cancer Cells. *Oncol Res*. 2017;25(3):455-461.
28. Du P, Luan X, Liao Y, et al. MicroRNA-509-3p inhibits cell proliferation and invasion via downregulation of X-linked inhibitor of apoptosis in glioma. *Oncol Lett*. 2018;15(1):1307-1312.
29. Zhang M, Zeng J, Zhao Z, Liu Z. Loss of MiR-424-3p, not miR-424-5p, confers chemoresistance through targeting YAP1 in non-small cell lung cancer. *Mol Carcinog*. 2017;56(3):821-832.
30. Lu T, Li Z, Yang Y, et al. The Hippo/YAP1 pathway interacts with FGFR1 signaling to maintain stemness in lung cancer. *Cancer Lett*. 2018;423:36-46.
31. Zhang MY, Lin J, Kui YC. MicroRNA-345 suppresses cell invasion and migration in non-small cell lung cancer by directly targeting YAP1. *Eur Rev Med Pharmacol Sci*. 2019;23(6):2436-2443.
32. Zou H, Wang S, Wang S, et al. SOX5 interacts with YAP1 to drive malignant potential of non-small cell lung cancer cells. *Am J Cancer Res*. 2018;8(5):866-878.
33. Zhang Y, Zhang Q, Chen H, Wang C. BCL9 promotes epithelial mesenchymal transition and invasion in cisplatin resistant NSCLC cells via beta-catenin pathway. *Life Sci*. 2018;208:284-294.

34. Wu Y, Hou Y, Xu P, et al. The prognostic value of YAP1 on clinical outcomes in human cancers. *Aging* (Albany NY). 2019;11.
35. Boivin GP, Bottomley MA, Schiml PA, Goss L, Grobe N. Physiologic, Behavioral, and Histologic Responses to Various Euthanasia Methods in C57BL/6NTac Male Mice. *Journal of the American Association for Laboratory Animal Science : JAALAS*. 2017;56(1):69-78.
36. Siegel RL, Miller KD, Jemal A. *Cancer Statistics, 2017*. CA: a cancer journal for clinicians. 2017;67(1):7-30.
37. Boolell V, Alamgeer M, Watkins DN, Ganju V. The Evolution of Therapies in Non-Small Cell Lung Cancer. *Cancers*. 2015;7(3):1815-1846.
38. Chang ZW, Jia YX, Zhang WJ, et al. LncRNA-TUSC7/miR-224 affected chemotherapy resistance of esophageal squamous cell carcinoma by competitively regulating DESC1. *Journal of experimental & clinical cancer research : CR*. 2018;37(1):56.
39. Fatica A, Bozzoni I. Long non-coding RNAs: new players in cell differentiation and development. *Nat Rev Genet*. 2014;15(1):7-21.
40. Du Z, Sun T, Haciosuleyman E, et al. Integrative analyses reveal a long noncoding RNA-mediated sponge regulatory network in prostate cancer. *Nature communications*. 2016;7:10982.
41. Wu C, Xu B, Yuan P, et al. Genome-wide interrogation identifies YAP1 variants associated with survival of small-cell lung cancer patients. *Cancer Res*. 2010;70(23):9721-9729.
42. Nishikawa E, Osada H, Okazaki Y, et al. miR-375 is activated by ASH1 and inhibits YAP1 in a lineage-dependent manner in lung cancer. *Cancer Res*. 2011;71(19):6165-6173.

Figures

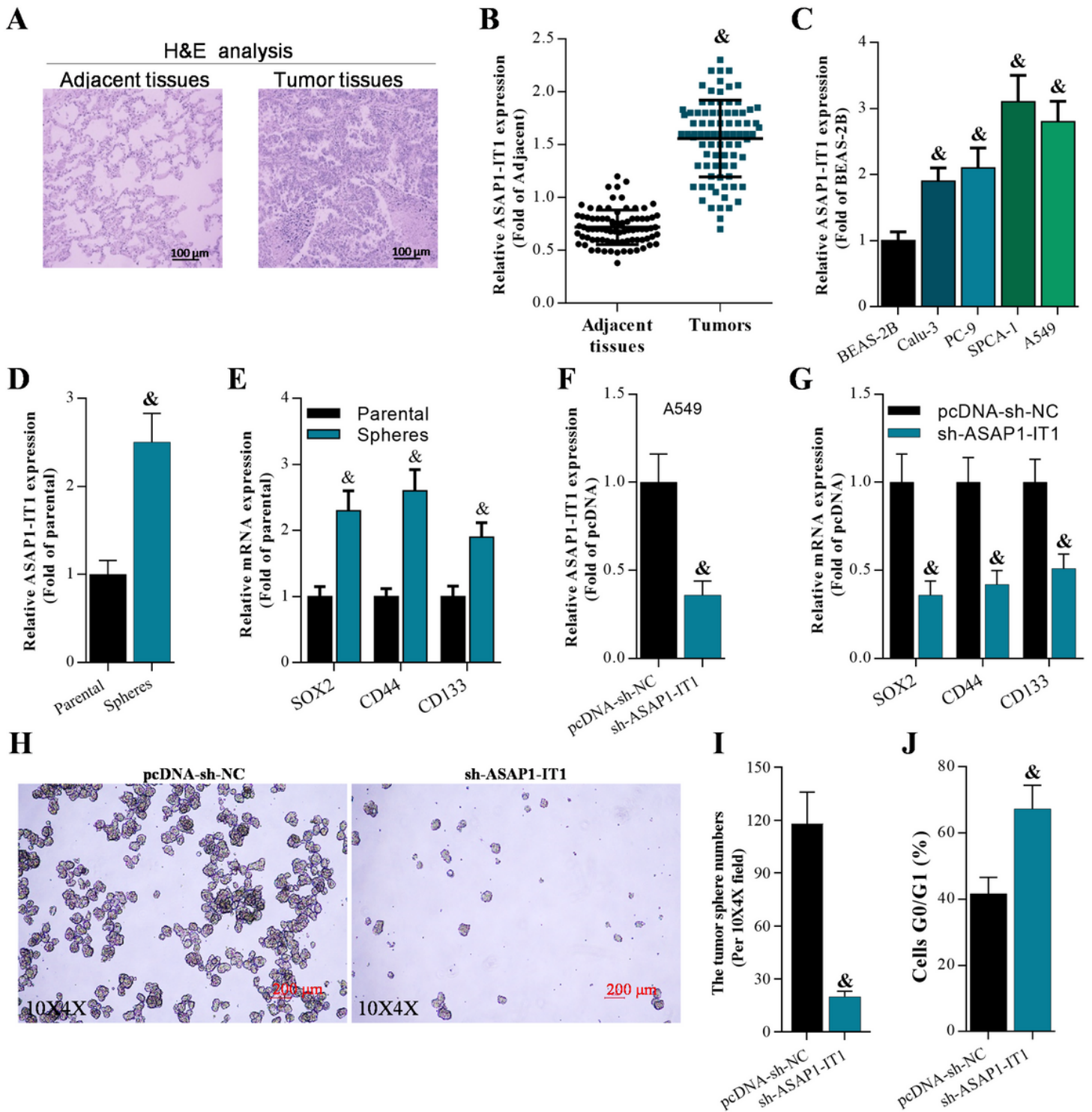


Figure 1

ASAP1-IT1 was elevated in NSCLC tissues and knockdown of ASAP1-IT1 inhibited stemness of NSCLC cells (A) H&E staining of NSCLC tissues and adjacent tissues. qRT-PCR analysis of ASAP1-IT1 expression in (B) NSCLC tissues and adjacent tissues, $& p < 0.01$ compared with adjacent tissues; (C) NSCLC cells and normal cells, $& p < 0.01$ compared with BEAS-2B cells; and (D) spheres of A549, $& p < 0.01$ compared with parental group. (E) qRT-PCR on the expression of stemness-associated genes (SOX2, CD44, and CD133) in stemness-enriched cell spheres and parental cells, $& p < 0.01$ compared with parental group. (F) qRT-PCR

analysis of ASAP1-IT1 levels after 48 h infection with pcDNA-sh-NC or pcDNA-sh-ASAP1-IT1 in A549-derived stem cells, &p<0.01 compared with pcDNA-sh-NC. (G) qRT-PCR analysis on stemness-associated gens (SOX2, CD44, and CD133) after 48 h infection with pcDNA-sh-NC or pcDNA-sh-ASAP1-IT1 in A549-derived stem cells, &p<0.01 compared with pcDNA-sh-NC. (H, I) Number of tumor spheres in ASAP1-IT1 knockdown A549-derived stem cells, &p<0.01 compared with pcDNA-sh-NC. (J) Flow cytometry analysis of cell cycle in A549 stem cells post 48 h infection, &p<0.01 compared with pcDNA-sh-NC.

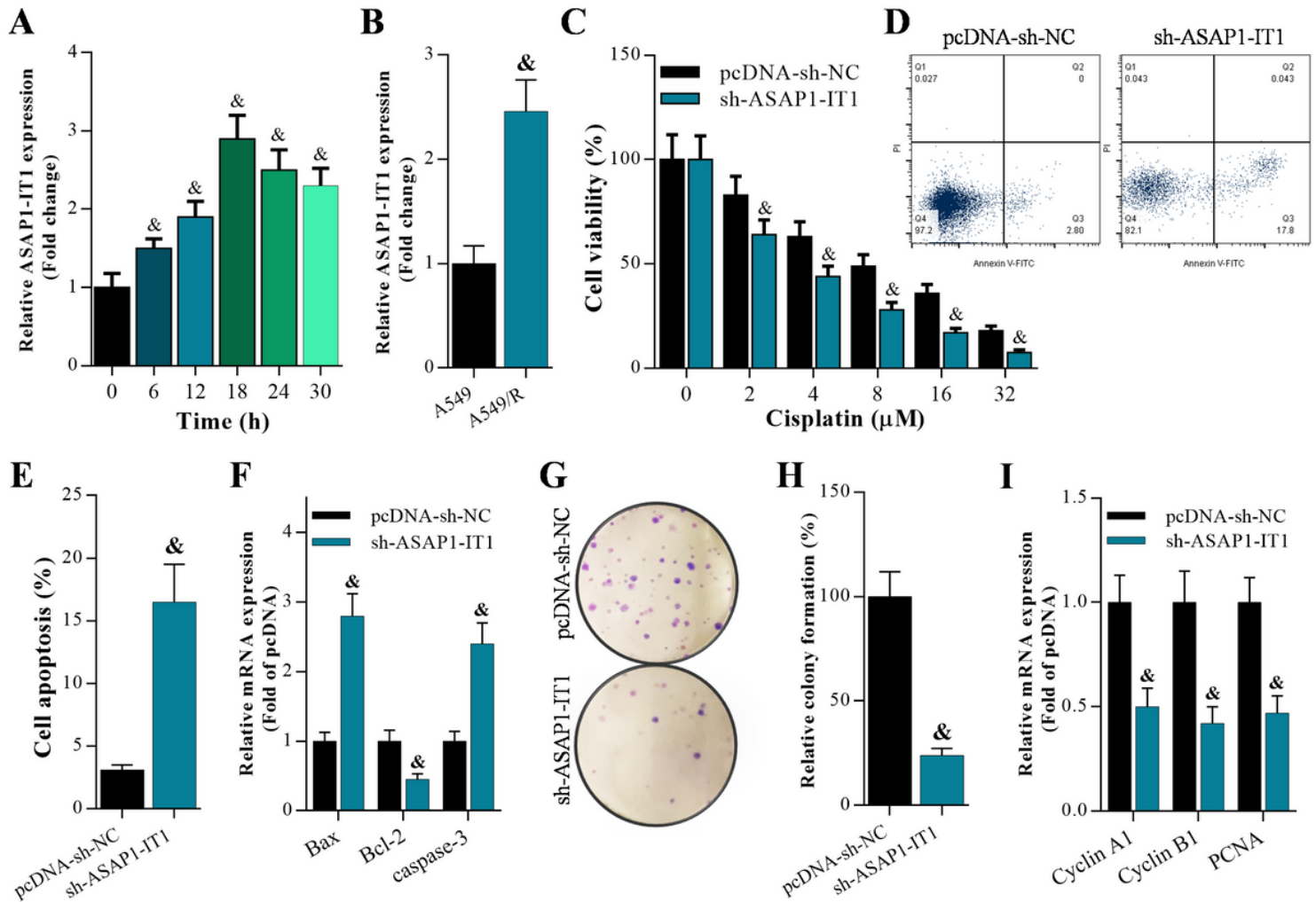


Figure 2

Knockdown of ASAP1-IT1 suppressed cisplatin resistance and cell growth of cancer stem cells and interfering ASAP1-IT1 promoted apoptosis qRT-PCR analysis of ASAP1-IT1 expression in (A) A549 cells post incubation with 4μM cisplatin at different times (0 h, 6 h, 12 h, 18 h, 24 h, 30 h), &p<0.01 compared with 0 h group and (B) A549 and cisplatin-resistant A549/R cells, &p<0.01 compared with A549. (C) CCK-8 assay on the cell viability of ASAP1-IT1 knockdown A549 cells incubated with cisplatin at various concentration (0 μM, 4 μM, 8 μM, 16 μM, 32 μM), &p<0.01 compared with pcDNA-sh-NC. (D, E) Annexin V-FITC/PI staining of A549-derived stem cells 48 h post infection, &p<0.01 compared with pcDNA-sh-NC. (F) qRT-PCR analysis of expression of apoptosis-associated genes (Bax, Bcl-2, caspase-3) 48 h after

infection in A549-derived stem cells, &p<0.01 compared with pcDNA-sh-NC. (G, H) Colony formation assay on cell growth of A549-derived stem cells after 15 days of culture, &p<0.01 compared with pcDNA-sh-NC. (I) qRT-PCR analysis on expression of proliferation-associated genes (Cyclin A1, Cyclin B1, and PCNA) after 48 h infection in A549-derived stem cells, &p<0.01 compared with pcDNA-sh-NC.

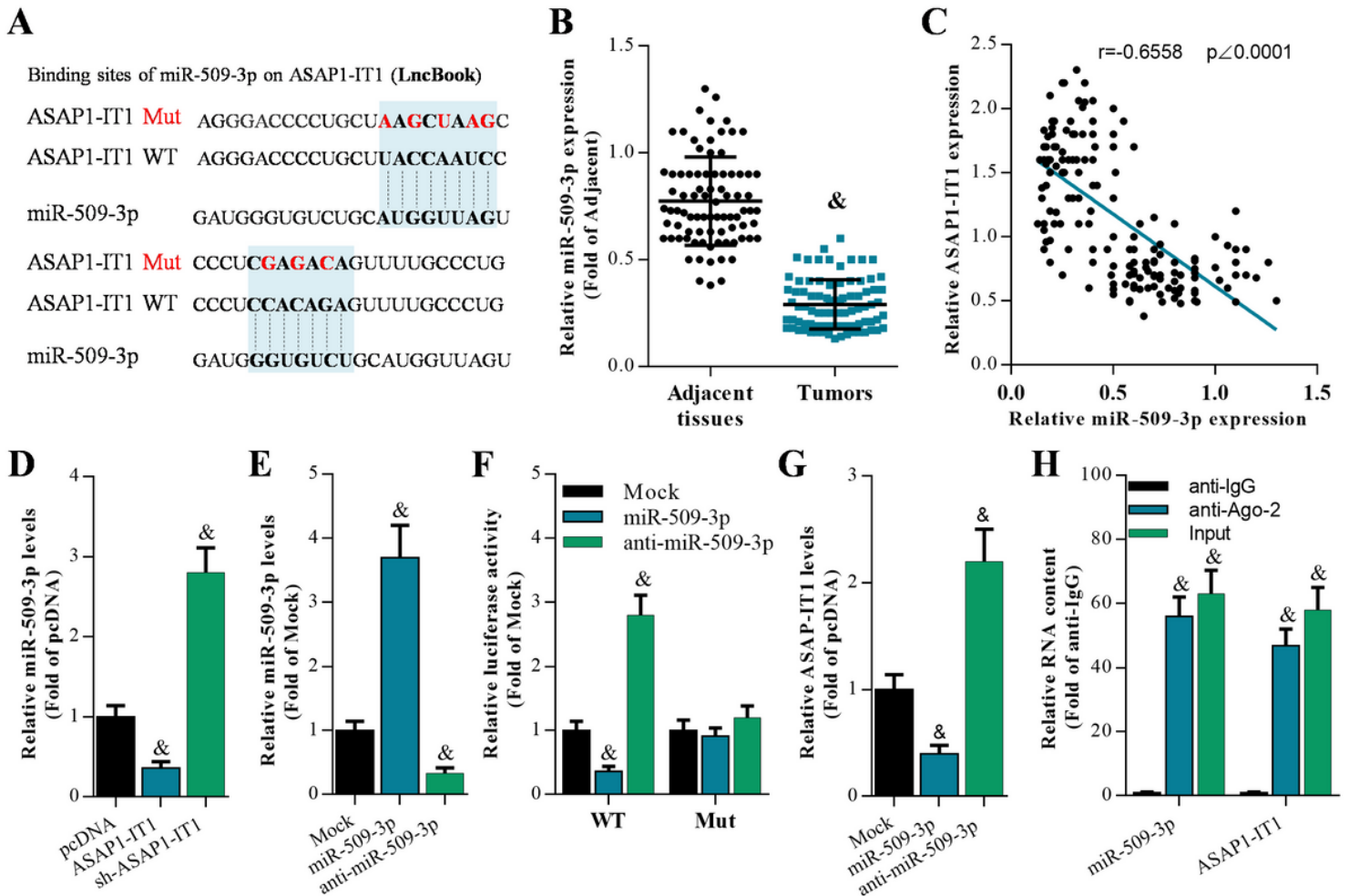


Figure 3

ASAP1-IT1 interacted with miR-509-3p (A) The potential binding sites of miR-509-3p on ASAP1-IT1 predicted by LncBook. (B) qRT-PCR analysis of miR-509-3p expression in NSCLC tissues and adjacent tissues, &p<0.01 compared with adjacent tissues. (C) The correlation of ASAP1-IT1 and miR-509-3p in clinical tissues. (D) qRT-PCR analysis of miR-509-3p in A549 cells 48h post infection with pcDNA, pcDNA-ASAP1-IT1 (ASAP1-IT1), and pcDNA-sh-ASAP1-IT1 (sh-ASAP1-IT1), &p<0.01 compared with pcDNA. (E) qRT-PCR analysis of miR-509-3p expression in A549 cells 48 h after transfection with mimic miRNAs, &p<0.01 compared with Mock. (F) Luciferase reporter assay on miR-509-3p on luciferase activity of pmirGLO-ASAP1-IT1 WT (wild type) and pmirGLO-ASAP1-IT1 Mut (mutant) 48 h post transfection with mimic miRNAs, &p<0.01 compared with Mock. (G) qRT-PCR analysis of ASAP1-IT1 expression in A549 cells 48 h after infection, &p<0.01 compared with Mock. (H) qRT-PCR analysis of RNA content after RIP assay in A549 cells, &p<0.01 compared with anti-IgG.

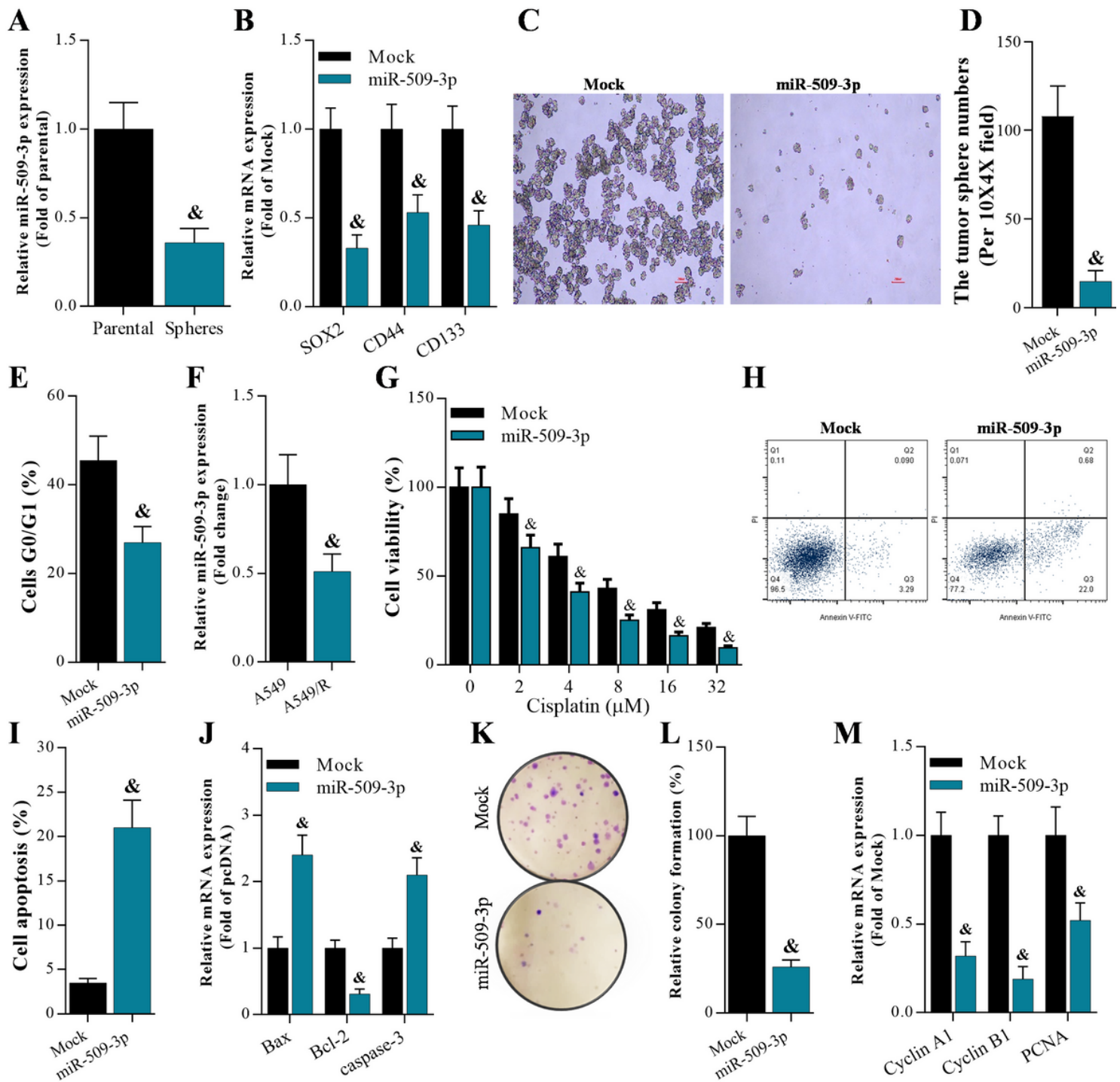


Figure 4

Overexpression of miR-509-3p inhibited stemness, cisplatin resistance and cell growth, and promoted apoptosis of A549-derived stem cells (A) qRT-PCR analysis on miR-509-3p in spheres of A549-derived stem cells, $&p < 0.01$ compared with parental group. (B) qRT-PCR on the expression of stemness-associated genes (SOX2, CD44, and CD133) in A549 cell spheres 48 h after transfection with mimic miRNAs, $&p < 0.01$ compared with Mock. (C, D) Number of tumor spheres in miR-509-3p overexpressing A549 stem cells, $&p < 0.01$ compared with Mock. (E) Flow cytometry analysis of cell cycle in A549-derived stem cells 48 h after overexpression of miR-509-3p, $&p < 0.01$ compared with Mock. (F) qRT-PCR analysis

of miR-509-3p in A549 and cisplatin-resistant A549/R cells. $p < 0.01$ compared with A549. (G) CCK-8 assay on the cell viability of miR-509-3p-overexpressing A549-derived stem cells treated with cisplatin at various concentration (0 μ M, 4 μ M, 8 μ M, 16 μ M, 32 μ M), $p < 0.01$ compared with Mock. (H, I) Annexin V-FITC/PI staining of A549-derived stem cells 48 h after miR-509-3p overexpression, $p < 0.01$ compared with Mock. (J) qRT-PCR analysis on expression of apoptosis-associated genes (Bax, Bcl-2, caspase-3) 48 h after transfection with miR-509-3p or Mock, $p < 0.01$ compared with Mock. (K, L) Colony formation assay on cell growth of A549-derived stem cells after 15 days culture, $p < 0.01$ compared with Mock. (M) qRT-PCR analysis on proliferation-associated genes (Cyclin A1, Cyclin B1, and PCNA) 48 h after overexpression of miR-509-3p in A549-derived stem cells, $p < 0.01$ compared with Mock.

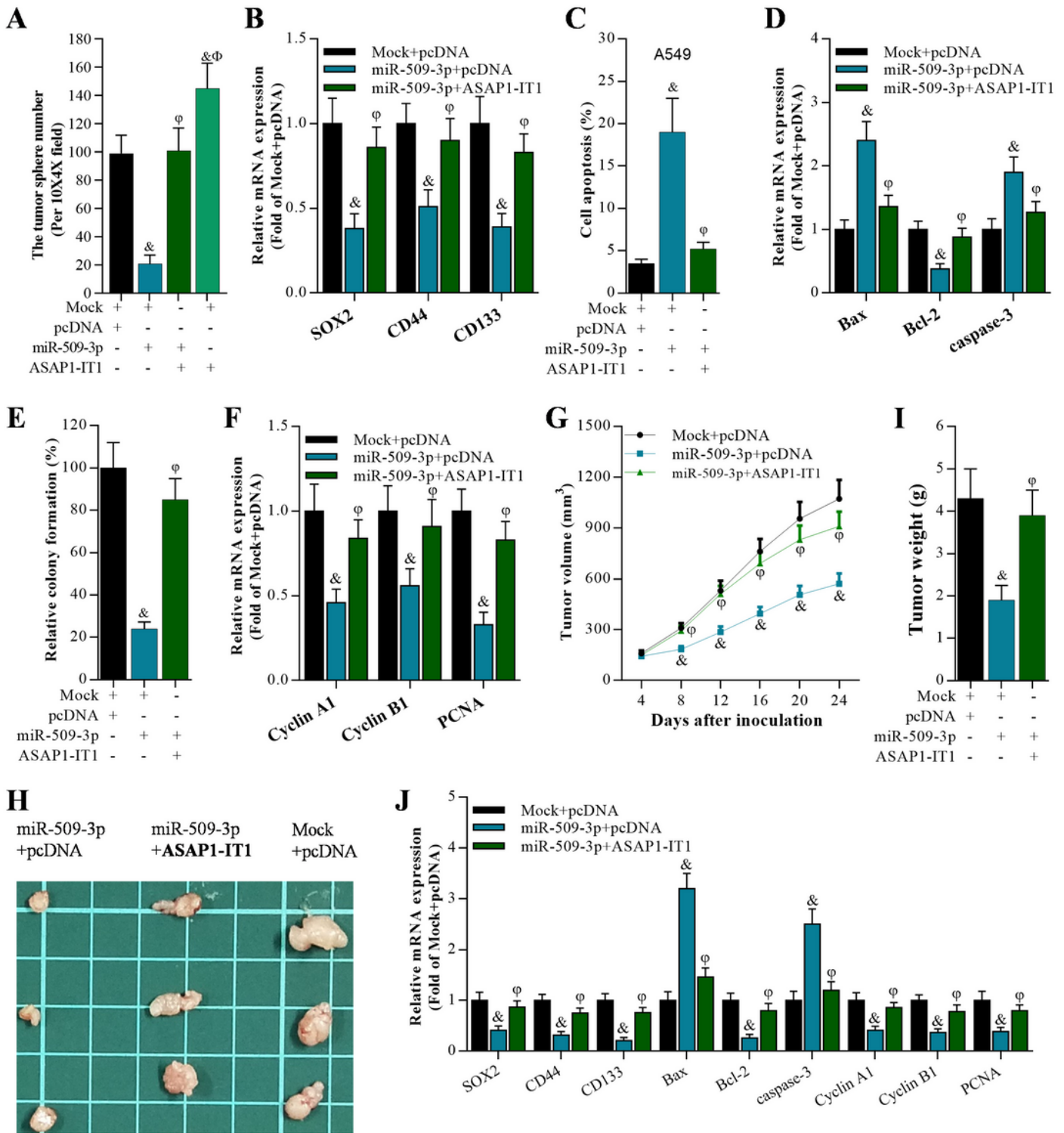


Figure 5

Overexpression of ASAP1-IT1 blocked miR-509-3p-mediated cell functions in cancer stem cells both in vitro and in vivo (A) Number of A549 cell tumor spheres after expression of Mock, pcDNA, miR-509-3p, and ASAP1-IT1, &p<0.01 compared with Mock+pcDNA, ϕ p<0.01 compared with miR-509-3p+pcDNA, Φ p<0.01 compared with miR-509-3p+ASAP1-IT1. (B) qRT-PCR analysis on stemness-related genes (SOX2, CD44, and CD133) in A549 stem cells, &p<0.01 compared with Mock+pcDNA,

parental group. (D) Luciferase activity of pmirGLO-YAP1-3'UTR-WT (wild type) or pmirGLO-YAP1-3'UTR-Mut (mutant) was modulated by miR-509-3p and ASAP1-IT1 in A549 cells, &p<0.01 compared with Mock+pcDNA, ϕ p<0.01 compared with miR-509-3p+pcDNA, Φ p<0.01 compared with miR-509-3p+ASAP1-IT1. (E) YAP1 mRNA levels in A549 cells analyzed by qRT-PCR, &p<0.01 compared with Mock+pcDNA, ϕ p<0.01 compared with miR-509-3p+pcDNA, Φ p<0.01 compared with miR-509-3p+ASAP1-IT1. (F) Western blot analysis on YAP1 protein in A549 cells.

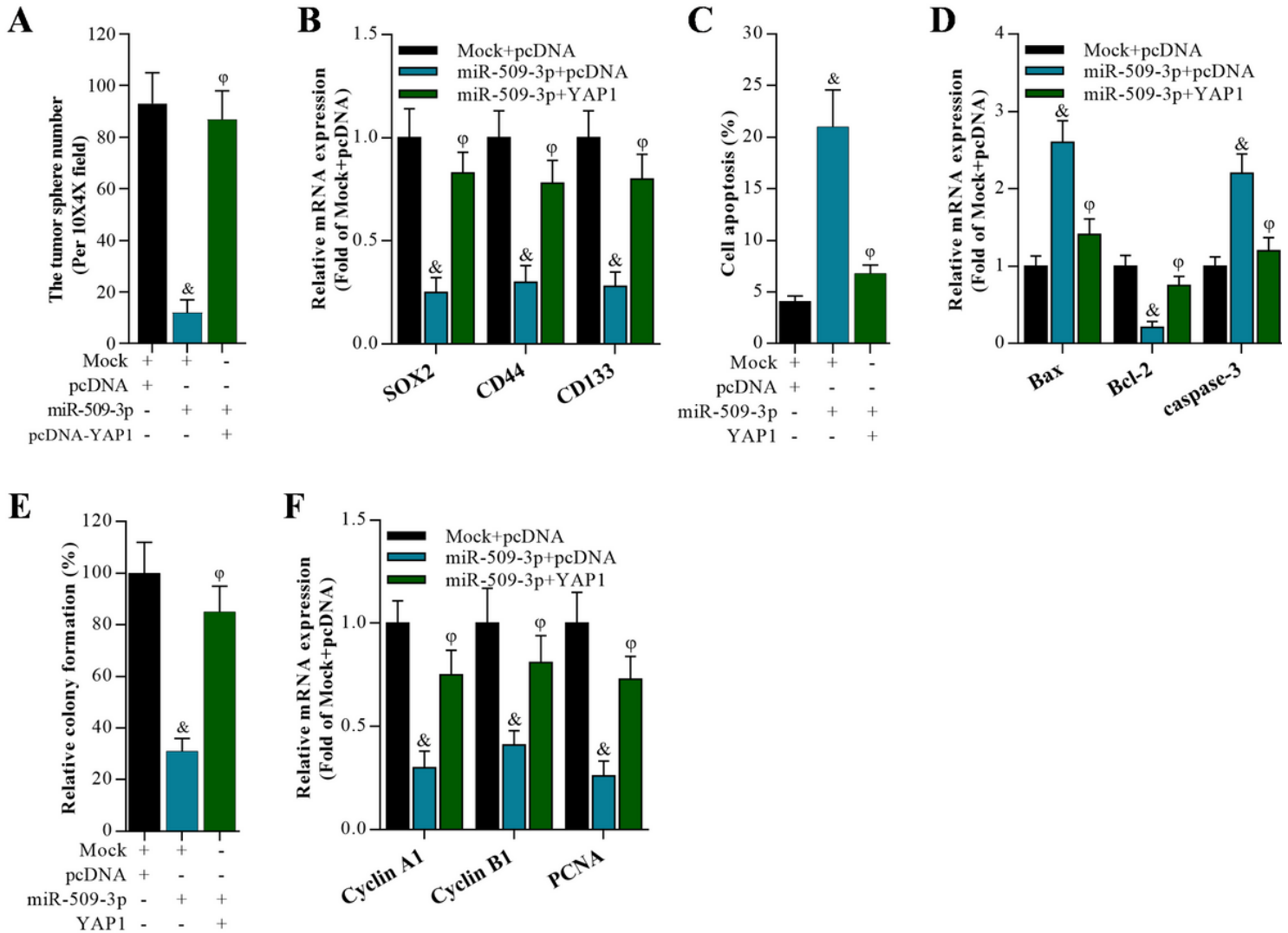


Figure 7

Overexpression of YAP1 reversed miR-509-3p-mediated cancer stemness, cell growth, and apoptosis of A549-derived stem cells (A) Number of tumor A549 spheres after transfection with Mock, pcDNA, miR-509-3p, and YAP1, &p<0.01 compared with Mock+pcDNA, ϕ p<0.01 compared with miR-509-3p+pcDNA. (B) qRT-PCR analysis on stemness-related genes (SOX2, CD44, and CD133) 48 h after transfection in A549-derived stem cells, &p<0.01 compared with Mock+pcDNA, ϕ p<0.01 compared with miR-509-3p+pcDNA. (C) Annexin V-FITC/PI staining of A549-derived stem cells after transfection with Mock, pcDNA, miR-509-3p, and YAP1, &p<0.01 compared with Mock+pcDNA, ϕ p<0.01 compared with miR-509-3p+pcDNA. (D)

qRT-PCR analysis on apoptosis-associated genes (Bax, Bcl-2, and caspase-3) in A549-derived stem cells, &p<0.01 compared with Mock+pcDNA, φp<0.01 compared with miR-509-3p+pcDNA. (E) Colony formation assay on cell growth of A549-derived stem cells after 15 days culture, &p<0.01 compared with Mock+pcDNA, φp<0.01 compared with miR-509-3p+pcDNA. (F) qRT-PCR analysis of growth-associated f genes (Cyclin A1, Cyclin B1, and PCNA) in stem cells of A549 cells, &p<0.01 compared with Mock+pcDNA, φp<0.01 compared with miR-509-3p+pcDNA.